



## Original Research Article

## Silymarin loaded solid lipid nanoparticles for oral delivery: Development, characterization and cytotoxic effect on breast cancer cells

Mohammad Akhlaquer Rahman<sup>1,\*</sup><sup>1</sup>Dept. of Pharmaceutics and Industrial Pharmacy, College of Pharmacy, Taif University, Taif, Saudi Arabia

## ARTICLE INFO

## Article history:

Received 22-04-2022

Accepted 10-05-2022

Available online 19-05-2022

## Keywords:

Silymarin  
Nanoparticles  
Solubility  
Cancer  
Cytotoxicity  
Stability

## ABSTRACT

**Aims:** The current study aimed to develop a silymarin (SM) loaded solid lipid nanoparticles (SLNs). Further, silymarin loaded solid lipid nanoparticles (SM-SLNs) were characterized for different quality parameters.

**Materials and Methods:** The SLNs were prepared by temperature modulated solidification technique. The glyceryl monostearate (GMS) was selected as lipid, tween 80 as surfactant and mannitol as cryoprotectant. The SM-SLNs were characterized for particle size, polydispersity index (PDI), zeta potential (ZP), entrapment efficiency (EE), thermal behavior, and crystallinity. Further, the formulation was elucidated by MTT assay for cytotoxicity assessment.

**Results:** The particle size and PDI of the optimized formulation was found to be  $178.6 \pm 4.32$  nm and 0.146, respectively. ZP (-36.4 mV) with a negative surface charge confirmed the physical stability of SLNs. Differential scanning calorimetry (DSC), X-ray diffraction (XRD) confirmed the transformation of lipid into SLNs through polymorphic transition of lipid crystallinity from  $\beta'$ -modification to  $\alpha$ -modification and conversion of crystallinity of drug to amorphous state. The optimized formulation had an EE of 79.86%. The in-vitro drug release depicted a burst release for 1 h followed by fast release for 6 h and then sustained release over a duration of 24 h. SM-SLNs significantly reduced the growth of MCF-7 cells compared to silymarin.

**Conclusion:** SM-SLNs exhibited small size in nanometer with narrow distribution, physically stable, and high entrapment efficiency. The developed nanoformulation could be used as a suitable drug delivery system for silymarin that has low water solubility, and a promising candidate for development of effective formulation in cancer therapy.

This is an Open Access (OA) journal, and articles are distributed under the terms of the [Creative Commons Attribution-NonCommercial-ShareAlike 4.0 License](https://creativecommons.org/licenses/by-nc-sa/4.0/), which allows others to remix, tweak, and build upon the work non-commercially, as long as appropriate credit is given and the new creations are licensed under the identical terms.

For reprints contact: [reprint@ipinnovative.com](mailto:reprint@ipinnovative.com)

## 1. Introduction

Breast cancer is the most common and leading cause of death among females in less developed countries.<sup>1</sup> Chemotherapy alone has been proven unsuccessful in the treatment of cancer due to the development of resistance in many cancer cell types.<sup>2,3</sup> As a result, novel agents with adequate therapeutic efficacy are needed. Silymarin (SM), a flavonolignan that is a bioactive

ingredient of *Silybum marianum* has chemosensitizing, antioxidant and anti-inflammatory properties. It also exhibits antineoplastic and cell-transporter altering, free radical scavenging, lipid peroxidation inhibitory, cellular membrane integrity enhancing, and steroid like effects as a phytochemical.<sup>4-6</sup> Recently, compounds from natural sources have been reported to suppress hyperproliferation, neoplastic transformation, and carcinogenesis.<sup>7</sup> Cancer research is focusing on phytochemicals as natural resource compounds and their potential for cancer prevention and/or treatment.<sup>8</sup> The antioxidant, anti-inflammatory

\* Corresponding author.

E-mail address: [rahmanpharma@gmail.com](mailto:rahmanpharma@gmail.com) (M. A. Rahman).

and proapoptotic properties are implying their anticancer efficacy.<sup>9</sup>

Solid lipid nanoparticles (SLNs) have emerged as a potential colloidal drug delivery system that combines the advantages of various traditional colloidal drug delivery systems while avoiding major shortcomings.<sup>10</sup> SLNs are formulated using solid lipids which are comparatively inexpensive and also physiologically safe as they fall under the generally recognized as safe (GRAS) category. Also, they possess better physical stability, good reproducibility and can be produced at comparatively lower costs.<sup>11</sup> In the present study, SLNs were formulated to successfully carry and deliver silymarin to the desired site with a sustained delivery. The feasibility of SLNs as a potential drug delivery system for silymarin was demonstrated through extensive characterization of various properties such as particle size, polydispersity index (PDI), zeta potential (ZP), entrapment efficiency (EE), differential scanning calorimetry (DSC), X-ray diffraction (XRD), drug release, and cytotoxic potential.

## 2. Materials and Methods

Silymarin was kindly donated as a gift sample from Ranbaxy, Gurgaon, India. Tween 80 was purchased from Merck India Ltd. Glyceryl monostearate (GSM) was generously provided by Gattefosse, France. Mannitol was supplied as a gift sample from Sigma Aldrich, Inc., USA. Dialysis membrane (MWCO:1200 g/mole) was purchased from HiMedia, Mumbai, India. Human breast adenocarcinoma cell line (MCF-7) purchased from the American Type Culture Collection. The other chemicals were of analytical reagent grade.

### 2.1. Solubility study for lipid selection

Solubility of silymarin in different lipids (dynasan 114, cetostearyl alcohol, glyceryl monostearate, palmitic acid, and stearic acid) were performed to select appropriate lipids by measuring the drug partitioning behavior between an aqueous and lipid phase. Briefly, 5 mg of the drug was weighed accurately and added to 10 ml of a water/lipid mixture in a glass bottle screw capped vial. All the vials were kept in a water bath maintained at 70°C for 1 h followed by cooling and centrifugation at 15,000 rpm for 15 min. The absorbance was taken using UV spectrophotometer (Ultrospec 210 pro, Amersham Biosciences, NJ) at 288 nm wavelength and the concentration of silymarin was determined utilizing standard plot. The lipid solubility of silymarin was calculated by subtraction of the aqueous layer concentration from the total amount of added drug and was expressed as a percentage.

### 2.2. Selection of surfactant

For the selection of appropriate surfactant in the formulation of SLNs, a fixed quantity of lipid (5%) was mixed with surfactant (3%) in aqueous solution at 70°C in a 10 ml volumetric flask. The mixture was vortexed for 5 min followed by sonication for 2 min and cooling in an ice bath and the resultant dispersion was examined for particle size, PDI, and ZP. Further, the preparation was left overnight at room temperature and observed for any precipitation under sufficient illuminated condition.

### 2.3. Preparation of silymarin loaded solid lipid nanoparticles

Silymarin loaded solid lipid nanoparticles (SM-SLNs) were prepared by temperature-modulated solidification method.<sup>11</sup> An appropriate amount of silymarin was added in a glass test tube previously kept in 1 g molten GSM and placed on a water bath shaker (Clifton, Nickel-Electro Ltd., North Somerset, UK) with temperature controlled at 75°C and speed at 1500 rpm for 48 h. Then, 2 g of tween 80 was added to it. The molten mixture was continuously heated in a water bath at a temperature not exceeding 80°C with intermittent vortexing every 5 min of heating for 20 s. The molten mixture was then added to the heated deionized water (80°C). The dispersion obtained was placed in an ice bath and homogenized at a speed of 4000 rpm for 45 min and then kept undisturbed on a bench top for 30 s. The dispersion was filtered using Amicon<sup>®</sup> Ultra Centrifugal filters (Ultracel<sup>®</sup>-100K) by subjecting it to centrifugation for 20 min. The residue obtained was re-suspended using 40 ml of deionized water. Suitable amount of mannitol was added to the dispersion obtained above and subjected for lyophilization for 72 h and used for further analysis.

### 2.4. Particle size analysis and polydispersity index

The particle size was determined by dynamic light scattering (Nicomp 380 ZLS, CA, USA) equipped with a 100mW He-Ne laser of wavelength 658 nm and a photodiode array detector. 1 mg of the lyophilized samples were re-dispersed in 10 ml of deionized water and vortexed at 3000 rpm for 5 min prior to measurement. The samples were then transferred to standard plastic cuvettes and analyzed at 23°C at an angle of 14.06° in the electrophoretic light scattering mode. Nicomp software was used for data acquisition and analysis. The particle size was obtained as z-average diameter and the PDI, a parameter for assessing the particle size distribution.

### 2.5. Measurement of zeta potential

Zeta potential measurement is important to assess the degree of charge present on suspended particles in dispersion which indicates the physical stability of the colloidal

disperse system. Sample for analysis was prepared by dispersing 1 mg of lyophilized product in 10 ml of deionized water and vortexed. The electrophoretic mobility of nanoparticles measured using a Malvern Zetasizer 4 (Malvern Instruments, UK) at a field strength of  $20 \text{ V cm}^{-1}$ .

## 2.6. Differential scanning calorimetry

The drug silymarin, solid lipid GMS, and SM-SLNs were studied for the thermal behavior using differential scanning calorimeter (DSC 131EVO, Setaram, Calorimetry, France). 5 mg of samples were placed in  $100 \mu\text{l}$  aluminum pans and crimped. An empty pan served as a reference. While recording the thermograms, heating rate of  $5^\circ\text{C}/\text{min}$  and a scanning range of 10 to  $200^\circ\text{C}$  were employed under nitrogen purging rate of 20 ml/min.

## 2.7. Powder x-ray diffraction

X-ray scattering measurements were performed on GMS alone, silymarin pure, and SM-SLNs, with a PANalytical's X-ray diffractometer (PANalytical's X'pert Pro Tokyo, Japan) equipped with X'Celerator high speed detector and Cu-K $\alpha$  source with a voltage of 45 kV, and a current of 40 mA. The samples were crushed, placed in an aluminum sample holder, and packed smoothly using a glass slide. The instrument was operated in the continuous scanning speed of  $4^\circ/\text{min}$  over a  $2\theta$  range of  $5^\circ$  to  $40^\circ$  and the results were evaluated using the X-Pert data collector version 2.1 software.

## 2.8. Drug entrapment efficiency

Approximately 5 mg of lyophilized SM-SLNs were solubilized in 10 ml of acetonitrile by vortexing at 3000 rpm for 2 min. The solution was then filtered through  $2 \mu\text{m}$  non-sterile membrane filter (Millipore, Ireland). The filtrate was analyzed for drug content spectrophotometrically at 288 nm wavelength using acetonitrile as blank. The EE of the drug was calculated using the following formula:

$$\% \text{ EE of silymarin} = \frac{\text{Practical silymarin content}}{\text{Theoretical Silymarin content}} \times 100$$

## 2.9. In vitro drug release study

The dialysis bag method was used to analyze the release of silymarin from lyophilized SM-SLNs. The dialysis bag was pretreated with dissolution media for 24 h. The lyophilized SM-SLNs equivalent to 140 mg silymarin were accurately weighed and placed in a sealed dialysis membrane (MWCO:1200 g/mole) with a molecular size cut off of 2500 Daltons. The dialysis membrane was placed in a dissolution apparatus II containing 900 ml simulated intestinal fluid and maintained at  $37^\circ\text{C} \pm 0.5^\circ\text{C}$ . Rotation of the paddle was set to 50 rpm. 1 ml of samples were collected

at regular time intervals i.e. 0.5, 1, 2, 4, 6, 8, 12 and 24 h, and replaced with fresh dissolution media. The amount of silymarin released was quantified spectrophotometrically at 288 nm.

## 2.10. Cytotoxicity study

The effect of silymarin on the viability of breast cancer cells was determined by 3-(4,5-dimethylthiazol-2-yl)-2,5-diphenyltetrazolium bromide (MTT) assay. A stock solution of silymarin was prepared in dimethyl sulfoxide (DMSO) with 1% final concentration. The free silymarin and SM-SLNs were suspended in fresh culture media and applied in different concentrations ranging from ( $2 \mu\text{M}$ - $150 \mu\text{M}$ ) on MCF-7 cells plated into 96-well plates ( $1 \times 10^5$  cells per well). The cells were incubated at  $37^\circ\text{C}$  in a humidified atmosphere of 5%  $\text{CO}_2$  in air and allowed to grow for 24 h. For MTT assay, the media was removed from all the wells,  $20 \mu\text{L}$  of 5 mg/ml MTT reagent was added to each well and the plates were kept in incubator for 4 h. After the incubation, the medium from each well was aspirated and the blue formazan crystals were solubilized in  $200 \mu\text{l}$  of DMSO, mixed thoroughly and kept at room temperature for 10 min. Plates were read on an ELISA reader at a wavelength of 570 nm. The value of absorbance is a measure of number of live cells. The corresponding values for optical density of different control, free drug and optimized formulation were recorded. The samples were run in triplicate ( $n=3$ ).

## 2.11. Stability study

The stability of lyophilized SM-SLNs were investigated at accelerated storage condition ( $40^\circ\text{C} \pm 2^\circ\text{C}/75\% \text{ RH} \pm 5\% \text{ RH}$ ) for 6 months. The sample was kept in amber colored glass container and placed in stability chamber. The sample was withdrawn at predetermined time interval and analyzed for particle size, PDI, ZP, EE and drug content.

## 3. Results and Discussion

### 3.1. Lipid and surfactant selection

In order to achieve maximum drug loading and entrapment efficiency, the solubility of silymarin in different lipids was evaluated. Glyceryl monostearate showed highest drug solubilizing ability with percent drug partitioned values of 72.43% followed by dynasan 114 (63.73%), cetostearyl alcohol (55.45%), palmitic acid (43.65%), and stearic acid (38.39%). Figure 1 depicts the solubility of silymarin in different lipids. For surfactant selection, SLN formulations alone were prepared using different surfactants and evaluated for particle size, PDI, ZP, and precipitation. As shown in Table 1, the tween 80-based SLNs had the smallest particle size ( $112.4 \pm 2.65 \text{ nm}$ ) and PDI (0.138), an optimum ZP (-35.6 mV). Moreover, the formulation did not show any signs of precipitation after the storage of 24 h.

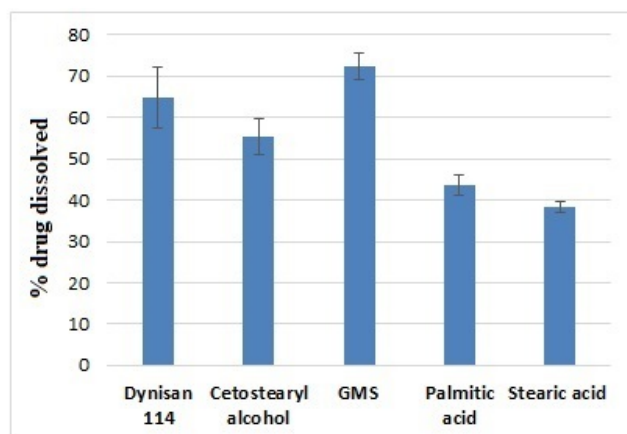


Fig. 1: Solubility of silymarin in various lipids.

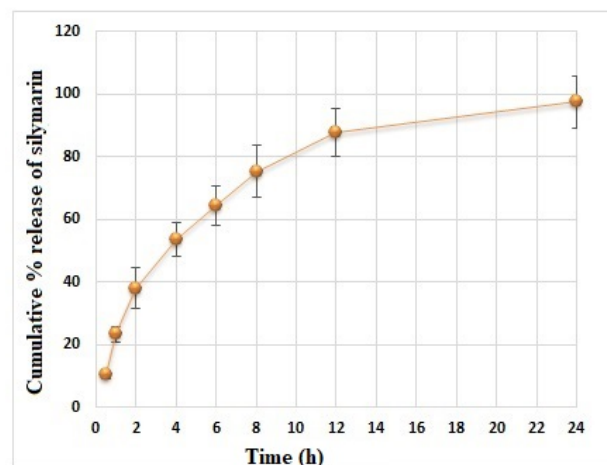


Fig. 3: In-vitro release profile of SM-SLNs in simulated intestinal fluid

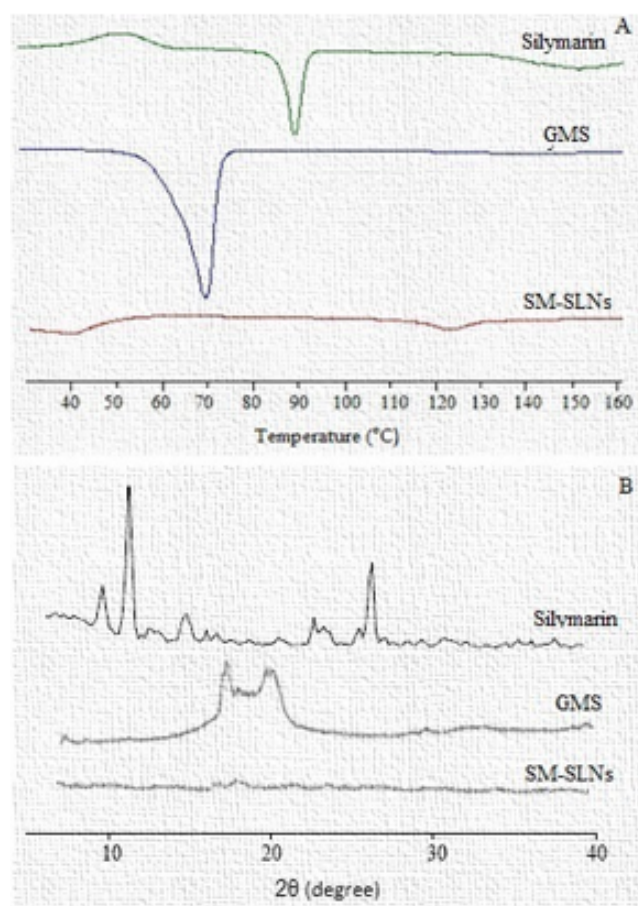


Fig. 2: DSC thermogram for silymarin, GMS, and SM-SLNs (A), and (B) XRD pattern of silymarin, GMS, and SM-SLNs.

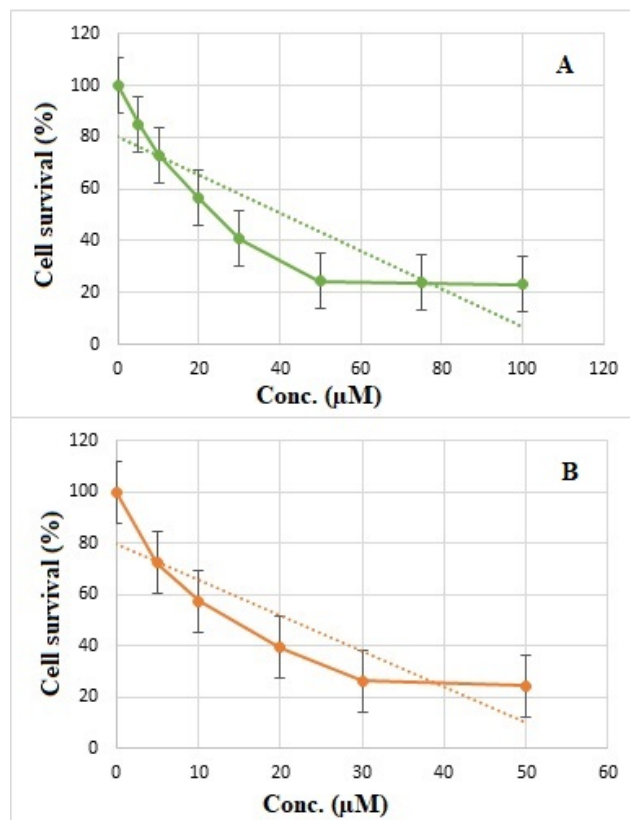


Fig. 4: Percentage survival of MCF-7 cells after treatment with (A) silymarin and (B) SM-SLNs

Hence, tween 80 was selected as suitable surfactant for SLN formulation.

### 3.2. Preparation of silymarin loaded solid lipid nanoparticles

Temperature modulated solidification technique involves the temperature of the surrounding environment with concurrent solidification and formation of lipid nanodispersion. The method is simple, free of any organic solvent and easy scale-up. GMS was used as lipid excipient and tween 80 as surfactant. Shear forces applied by high-speed homogenization followed by sudden cooling lead to formation of the SLN. Tween 80 reduces the interfacial tension between the molten lipid and the aqueous phase. The temperature was reduced with simultaneous homogenization leading to the formation of SLN. The formulation was optimized by varying drug/lipid ratio, surfactant concentration and the emulsification time. With increase in lipid concentration, the particle size increases. The increase in particle size was observed after reaching the threshold value of lipid in the formulation.<sup>12</sup> To limit the surfactant-based toxicity in cell cultures and animal tissues, a minimum possible amount of surfactant was used in the optimized formulation with a lipid/surfactant ratio of 1:2. Aqueous dispersions have poor stability making it necessary to utilize special handling and storage conditions. Lyophilization is good solution to transform aqueous dispersions into solid forms to enhance the stability.<sup>13</sup> Freeze drying causes aggregation and irreversible fusion of nanoparticles leading to destabilization. Hence, cryoprotectants are added before freezing, protects the formulation from freezing stress.<sup>14</sup> Mannitol was selected as the cryoprotectant after trying sucrose, mannitol and trehalose in the formulation and subsequently evaluating the particle size of the lyophilized SLNs. Optimized formulation composed of lipid to mannitol ration 1:1.

### 3.3. Particle size analysis and polydispersity index

The particle size of SLNs was analyzed before and after lyophilization. An increase in average particle size was observed after lyophilization process. Despite use of cryoprotectants, an increase in particle diameter has been observed after lyophilization.<sup>15</sup> Particle size increase after lyophilization may be attributed to the use of lesser volume of redispersion media compared to that used during preparation leading to an increase in SLN concentration and interparticulate interaction favoring aggregation to form larger structures. In addition, cryoprotectant may deposit on the surface of the SLNs further increasing the overall particle diameter.<sup>11</sup> The average particle size of SM-SLNs measured before and after lyophilization was found to be  $112.4 \pm 2.65$  nm and  $178.6 \pm 4.32$  nm, respectively.

### 3.4. Zeta potential measurement

The ZP measurements were performed for lyophilized SM-SLNs. All the obtained ZP values were negative in charge because of the presence of glyceryl monostearate which is a fatty acid ester.<sup>16</sup> ZP is a major factor to evaluate the stability of any colloidal dispersion.<sup>17</sup> Stable dispersion of particles is possible when the absolute value of ZP is above 30 mV (both negative and positive) because of the repulsions produced by the surface electric charge of the particles in the dispersion.<sup>18</sup> Lower ZP values may lead to interparticulate interaction resulting in flocculation and coagulation. As the obtained ZP values for SM-SLNs were over negative 30 mV, the SLNs were found to be physically stable.

### 3.5. Differential scanning calorimetry

The DSC gives information about the melting and recrystallization behavior of crystalline material and is therefore used to evaluate the polymorphism and/or interactions between the lipid and the drug. The GMS exhibited a sharp endothermic peak of 71°C and glass transition temperature of 67°C. The SLNs melted at comparable temperature and exhibited melting peaks approximately 8 degrees lower than that of the pure lipid (Figure 2A). This indicates a transformation of the lipid into nanoparticles through polymorphic transition of lipid crystallinity from  $\beta'$ -modification to  $\alpha$ -modification.<sup>19,20</sup> The degree of crystallinity is reduced and also the melting enthalpy is decreased with the formation of nanoparticles. A wide endothermic peak was observed in the DSC thermogram of pure silymarin at about 90°C, and a glass transition temperature of 70°C.<sup>21</sup> The DSC thermo gram of SM-SLNs did not exhibit a peak at or around 90°C indicating either the successful conversion of crystalline silymarin into amorphous form in the SLNs or drug being successfully dispersed into the melted matrix of GMS.<sup>22</sup>

### 3.6. Powder x-ray diffraction

Powder X-ray diffraction patterns were analyzed to study the solid-state nature of the SLNs. The diffraction patterns of the lyophilized SM-SLNs were compared with that of the pure silymarin and pure GMS, respectively (Figure 2B). Silymarin diffractogram exhibited sharp and high intensity peaks. These peaks were either of very low intensity, less sharp, or completely absent in the diffractogram of SM-SLNs. This indicates that silymarin is present in its amorphous form in the SLNs. Broad and high intensity peaks were displayed at  $2\theta$  equals 19.54 and 23.46° by pure GMS. These two characteristic peaks of GMS were not prominently observed in the XRD patterns of SM-SLNs indicating decreased crystallinity of GMS in SLNs.<sup>23</sup> The XRD results support data obtained from DSC.

**Table 1:** Preparation of preliminary SLNs for selection of surfactant.

Lipid	Surfactant	Particle size (nm)	PDI	ZP (mV)	Precipitation (after 24 h )
Glyceryl monostearate	Pluronic F 68	193.8 ± 4.63	0.375	-26.3	No precipitation
	Transcutol P	168.2 ± 3.18	0.296	-27.5	Slight precipitation
	Solutol HS15	175.3 ± 4.08	0.249	-28.7	No precipitation
	Tween 80	112.4 ± 2.65	0.138	-35.6	No precipitation
	Labrasol	157.8 ± 2.94	0.274	-31.2	Slight precipitation
	Cremophor RH 40	145.6 ± 3.24	0.286	-30.5	Slight precipitation

**Table 2:** IC<sub>50</sub> % death of MCF-7 cells at minimum and maximum concentration of silymarin.

Test sample	Conc. (min)	% Death	Conc. (max)	% Death	IC <sub>50</sub>
Silymarin	5 μM	13.46 ± 0.37	50 μM	78.37 ± 2.26	27.23 ± 1.76
SM-loaded SLNs	5 μM	28.86 ± 1.56	50 μM	78.53 ± 3.14	16.45 ± 1.62

**Table 3:** Results of stability study.

Months	Particle size (nm)	PDI	ZP (mV)	EE (%)	Drug content (%)
0	178.6 ± 4.32	0.146	-36.4	79.86 ± 3.56	100.0
1	178.8 ± 2.55	0.146	-36.2	80.23 ± 3.56	99.87
2	179.0 ± 3.18	0.148	-35.6	80.86 ± 3.56	99.42
3	181.4 ± 5.06	0.152	-34.3	82.18 ± 3.56	99.11
4	181.7 ± 3.78	0.156	-34.1	84.15 ± 3.56	99.00
5	183.9 ± 5.03	0.156	-34.1	84.26 ± 3.56	98.75
6	186.2 ± 4.17	0.159	-33.8	87.21 ± 3.56	98.32

### 3.7. Drug entrapment efficiency

The entrapment efficiency of SLNs before and after lyophilization were  $72.42 \pm 2.43$  and  $79.86 \pm 3.56\%$ , respectively. High-encapsulation efficiency observed advocates the lipophilic nature of silymarin. Cryoprotectant plays an important role in EE of SLNs and a remarkable effect has been observed in the result. Addition of mannitol during lyophilization causes slight increase in EE. GMS was the lipid used in this formulation. GMS is a monoglyceride that creates an ordered solid lipid matrix leading to reduced number of imperfections in the SLN structure. This leads to reduced space to accommodate drug molecules in the crystal lattice.<sup>11</sup>

### 3.8. In vitro release

The in-vitro drug release profile of SM-SLNs is shown in (Figure 3). The SLNs showed a biphasic release pattern with an initial burst release in the first 1 h releasing approximately 23% of drug followed by fast release up to 6 hrs and subsequent sustained release for a period of 24 h. A maximum of approximately 97% of drug release was obtained from the SLNs. This release profile may be explained based on the partition effects of the drug between molten lipid and water phase during the homogenization step in the formulation procedure. During this step, hot water is used which is gradually cooled in an ice bath with simultaneous homogenization. As the temperature of the water gradually drops, the solubility of drug in water decreases which leads to re-partitioning of the drug into the

lipid phase. As the recrystallization temperature of the lipid is reached, a solid core starts forming including the drug present in lipid phase at this temperature. Further decrease in the temperature imposes more pressure on the drug to re-partition into the lipid phase as its aqueous solubility further decreases. However, the already formed lipid core cannot take up anymore drug consequently leading to increased concentration of drug in the outer shell or surface of the SLNs. The sustained release of silymarin can be utilized to prolong the drug release subsequently reducing the frequency of drug administration.

### 3.9. Cytotoxicity study

Cancer therapy by using the classical chemotherapeutics has too many side effects also exhibit high level of toxicity for patients. Novel approaches on cancer therapy imply the use of phytochemicals and/or other nanoscale sized natural products that offer low toxicity and fewer side effects. These nano formulations are more effective in low doses than the normal sized agents in cancer treatment. The treatment with nanoparticles led to the inhibition of the growth of MCF-7 cells. It was observed that after 24 h of MTT assay, silymarin in suspension form were cytotoxic, showing linear relationship between concentrations of drugs vs cell death. A cell death of  $13.46 \pm 0.37\%$  and  $78.37 \pm 2.26\%$  were observed at the lowest and highest concentration of silymarin, respectively (Table 2). The IC<sub>50</sub> values were calculated by interpolating the graph between % cell survival and concentration of drugs at 50% cell survival.

The IC<sub>50</sub> value for silymarin was calculated to be 27.23 ± 1.76 μM (Figure 4A). While, a maximum cell death of 78.53 ± 3.14% and minimum cell death of 28.86 ± 1.56% was observed at 50 and 5 μM concentration of silymarin from SLNs (Table 2). The IC<sub>50</sub> value was calculated to be 16.45 ± 1.62 μM (Figure 4B). Over all, the SM-SLNs was observed more effective at lower doses in causing cell death and exhibited maximum cytotoxicity. The IC<sub>50</sub> of SLN was less than the pure silymarin. The results demonstrated that silymarin carried by SLNs to the cells is much more effective than free silymarin. This may be attributed to the fact that small size of the nanoparticles facilitates their uptake by the cells.

### 3.10. Stability study

The results of stability studies are mentioned in Table 3. After 6 months of storage, there was insignificant variation in the particle size, PDI, ZP, and EE of SLNs. Further, less than 2% variation in the content uniformity of the silymarin from SM-SLNs demonstrated the stability of developed formulation.

## 4. Conclusion

Silymarin loaded SLNs were successfully developed by cost effective temperature modulated solidification technique. The nanoparticles demonstrated the particle size in nanometer, narrow size distribution, sufficiently stable and high entrapment efficiency of silymarin. SLNs developed was considered as a solution for eliminating the limitations of silymarin. Research findings suggest that both silymarin and SM-SLNs have been cytotoxic under breast cancer cells in dose dependent manner, latter being more effective. The results suggest that the developed nanoparticles may be used as a potential medication for anticancer therapy.

## 5. Source of Funding

None.

## 6. Conflicts of Interest

None.

## References

- Torre LA, Bray F, Siegel RL, Ferlay J, Tieuvent JL, Ahmedin J. Global cancer statistics. *CA Cancer J Clin.* 2015;61(2):87–108. doi:10.3322/caac.20107.
- Liu RH. Potential synergy of phytochemicals in cancer prevention: mechanism of action. *J Nutr.* 2004;134(12):3479–85. doi:10.1093/jn/134.12.3479S.
- Obradovic A, Zizic J, Trisovic N, Bozic J, Uscumlic G, Bozic B. Evaluation of antioxidative effects of twelve 3-substituted-5,5-diphenylhydantoin on human colon cancer cell line HCT-116. *Turk J Biol.* 2013;37(1):741–7. doi:10.3906/biy-1302-15.
- Karimi G, Vahabzadeh M, Lari P, Rashedinia M, Moshiri M. Silymarin, a promising pharmacological agent for treatment of diseases. *Iran J Basic med Sci.* 2011;14(2):308–17.
- Prasad NR, Muthusamy G, Shanmugam M, Ambudkar SV. South Asian medicinal compounds as modulators of resistance to chemotherapy and radiotherapy. *Cancers (Basel).* 2016;8(3):32. doi:10.3390/cancers8030032.
- Montgomery A, Adeyeni T, San K, Heuertz RM, Ezekiel RU. Curcumin sensitizes silymarin to exert synergistic anticancer activity in colon cancer cells. *J Cancer.* 2016;7(10):1250–7. doi:10.7150/jca.15690.
- Agarwal R, Agarwal C, Ichikawa H, Singh RP, Aggarwal BB. Anticancer potential of silymarin: From bench to bed side. *Anticancer Res.* 2006;26(6B):4457–98.
- Aljuffali IA, Fang CL, Chen CH, Fang JY. Nanomedicine as a strategy for natural compound delivery to prevent and treat cancers. *Curr Pharm Design.* 2016;22(27):4219–31. doi:10.2174/1381612822666160620072539.
- Iriti M, Faoro F. Bioactivity of grape chemicals for human health. *Nat Prod Commun.* 2009;4(5):611–34. doi:10.1177/1934578X0900400502.
- Muller RH, Mader K, Gohla S. Solid lipid nanoparticles (SLN) for controlled drug delivery—a review of the state of the art. *Eur J Pharm Biopharm.* 2000;50(1):161–77. doi:10.1016/s0939-6411(00)00087-4.
- Lakkadwala S, Nguyen S, Lawrence J, Nauli SM, Nesamony J. Physico-chemical characterisation, cytotoxic activity, and biocompatibility studies of tamoxifen-loaded solid lipid nanoparticles prepared via a temperature-modulated solidification method. *J Microencapsul.* 2014;31(6):590–9. doi:10.3109/02652048.2014.898707.
- Zhang J, Fan Y, Smith E. Experimental design for the optimization of lipid nanoparticles. *J Pharm Sci.* 2009;98(5):1813–9. doi:10.1002/jps.21549.
- PRodríguez AD, Solinis MA, Gascon AR, Pedraz JL. Short-and long-term stability study of lyophilized solid lipid nanoparticles for gene therapy. *Eur J Pharm Biopharm.* 2009;71(2):181–9. doi:10.1016/j.ejpb.2008.09.015.
- Pardeshi C, Rajput P, Belgamwar V, Tekade A, Patil G, Chaudhary K, et al. Solid lipid based nanocarriers: an overview. *Acta Pharm.* 2012;62(4):433–72. doi:10.2478/v10007-012-0040-z.
- Yang SC, Zhu JB. Preparation and characterization of camptothecin solid lipid nanoparticles. *Drug Dev Ind Pharm.* 2002;28(3):265–74. doi:10.1081/ddc-120002842.
- Hu L, Xing Q, Meng J, Shang C. Preparation and enhanced oral bioavailability of cryptotanshinone-loaded solid lipid nanoparticles. *AAPS PharmSciTech.* 2010;11(2):582–7. doi:10.1208/s12249-010-9410-3.
- Liu J, Gong T, Wang C, Zhong Z, Zhang Z. Solid lipid nanoparticles loaded with insulin by sodium cholate-phosphatidylcholine-based mixed micelles: preparation and characterization. *Int J Pharm.* 2007;340(1):153–62. doi:10.1016/j.ijpharm.2007.03.009.
- Muller R, Jacobs C, Kayser O. Nanosuspensions as particulate drug formulations in therapy: rationale for development and what we can expect for the future. *Adv Drug Deliv Rev.* 2001;47(1):3–19. doi:10.1016/s0169-409x(00)00118-6.
- Kuntsche J, Horst JC, Bunjes H. Cryogenic transmission electron microscopy (cryo-TEM) for studying the morphology of colloidal drug delivery systems. *Int J Pharm.* 2011;417(1):120–37. doi:10.1016/j.ijpharm.2011.02.001.
- Zimmermann E, Souto E, Müller R. Physicochemical investigations on the structure of drug-free and drug-loaded solid lipid nanoparticles (SLN) by means of DSC and <sup>1</sup>H NMR. *Pharmazie.* 2005;60(7):508–13.
- Li Z, Yu L, Zheng L, Geng F. Studies on crystallinity state of puerarin loaded solid lipid nanoparticles prepared by double emulsion method. *J Therm Anal Calorim.* 2010;99(2):689–93. doi:10.1007/s10973-009-0127-z.
- Rahman Z, Zidan AS, Khan MA. Non-destructive methods of characterization of risperidone solid lipid nanoparticles. *Eur J Pharm Biopharm.* 2010;76(1):127–37. doi:10.1016/j.ejpb.2010.05.003.
- Feng F, Zheng D, Zhang D, Duan C, Wang Y, Jia L, et al. Preparation, characterization and biodistribution of nanostructured lipid carriers for

parenteral delivery of bifendate. *J Microencapsul.* 2011;28(4):280–5.  
doi:10.3109/02652048.2011.559285.

**Cite this article:** Rahman MA. Silymarin loaded solid lipid nanoparticles for oral delivery: Development, characterization and cytotoxic effect on breast cancer cells. *Curr Trends Pharm Pharm Chem* 2022;4(2):75-82.

### Author biography

**Mohammad Akhlaquer Rahman**, Assistant Professor